**Proceedings of ASME 2009 International Design Engineering Technical Conferences &
Computers and Information in Engineering Conference
IDETC/CIE 2009
August 30 – September 2, 2009, San Diego, California, USA**

DETC2009/DAC-87101

METAMORPHOSIS OF PERIODIC SURFACE MODELS

Cheng Qi and Yan Wang
Department of Industrial Engineering & Management Systems
University of Central Florida
Orlando, FL 32816

ABSTRACT

A phase transition is a geometric and topological transformation process of materials from one phase to another, each of which has a unique and homogeneous physical property. Providing an initial guess of transition path for further physical simulation studies is highly desirable in materials design. In this paper, we present a metamorphosis scheme for periodic surface (PS) models by interpolation in the PS parameter space. The proposed approach creates multiple potential transition paths for further selection based on three smoothness criteria. The goal is to search for a smooth transformation in phase transition analysis.

1. INTRODUCTION

Computer-aided nano-design (CAND) is an extension of computer based engineering design traditionally at bulk scales to nano scales. The general target of modeling and simulation in nanomaterial design is to search stable and realizable structures and conformations with the minimal total system energy. Geometry optimization is the central theme in most of the nanoscale simulations. For the widely used local search algorithms, simulation results are sensitively dependent on the initial conformation. Modeling methods, which allow for the efficient construction of initial geometries that are reasonably close to global optimal solutions, are important to improve both convergence rate and accuracy of prediction. Thus, enabling efficient structural description and editing is one of the key research issues in CAND. In the previous research [1, 2], an implicit surface modeling approach known as periodic surface (PS) model is proposed. Periodic surfaces are either loci or foci. Loci surfaces are fictional continuous surfaces that pass through discrete particles in 3D space, whereas foci surfaces can be looked as isosurfaces of potential or density in which discrete particles are enclosed. The PS model allows for parametric construction from atomic scale to meso scale. Reconstruction of loci surfaces from crystals [3], surface degree operations to support fine-grained modeling [4, 5], and feature-based approach for crystal construction [6, 7] were also studied.

In this paper, we propose a surface morphing or metamorphosis approach for PS models. This geometry transformation is very useful to simulate and visualize phase transition processes in studying functional materials. A phase transition is a geometric and topological transformation process of materials from one phase to another, each of which has a unique and homogeneous physical property [8, 9]. Transformation of PS models can help to visualize structure changes and provide initial estimations of transition paths. For example, Figure 1(a) shows a $BaSi_2$ structure in its cubic phase and the corresponding foci surface model, which encloses Ba atoms. It has properties of semi-conductor. Figure 1 (b) shows a layered phase of $BaSi_2$, which has properties of metal. The interest of phase transition analysis is to search the global optimal transition path between the two phases with the minimal potential energy change. Structure transformation based on geometric analysis such as the one in Figure 2 can provide an initial guess of transition path for further physical simulation studies. In this paper, the type of phase transition which we are interested in is the movement of many atoms that results in a continuous change between two different crystal structures. The examples of such type of phase transition can be diffusionless transformations and martensitic transformation. Any other types of phase transition such as a melting transformation or a freezing transformation are not in the scope of this paper. We reasonably assume that the transition between two phases is processed in a region where all the physical conditions in that region are uniformly distributed. Hence, we ignore the influence of physical treatments such as temperatures and pressures, and only focus on the metamorphosis of geometry itself.

A surface morphing approach for PS models is proposed in this paper. Three smoothness criteria are proposed to quantify structure changes for pathway selection. The main contribution of this paper is the unique surface morphing method of our PS model based on interpolation in the PS parameter space. Our method can provide multiple potential transition paths for choices with different criteria.

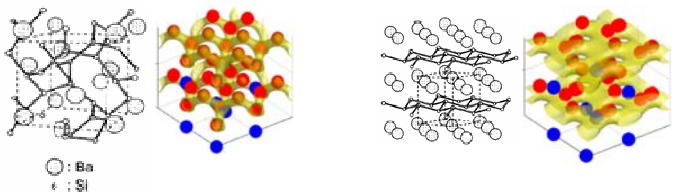

(a) $BaSi_2$ structures in cubic phase (b) $BaSi_2$ structures in layer phase

Figure 1. $BaSi_2$ and corresponding foci surfaces

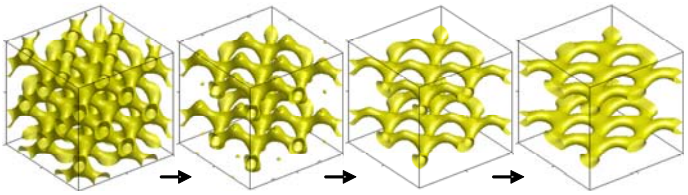

Figure 2. Foci surface transition from $BaSi_2$ cubic phase to layer phase

In the remainder of the paper, Section 2 gives a brief overview of related work in surface morphing with implicit and volumetric representations. Section 3 reviews the basis of the periodic surface model and its matrix form. Section 4 describes two surface morphing schemes, which are direct linear interpolation and interpolation in the PS parameters space. Section 5 proposes three smoothness criteria for choosing surface morphing paths.

2. 3D METAMORPHOSIS OF IMPLICIT SURFACES

Research effects in metamorphosis initially focused on two dimensional images. For image morphing, there have been extensive investigations [10, 11, 12]. A direct extension from 2D metamorphism to 3D was proposed by Mittal [13]. The 3D objects were represented by multiple 2D images and 2D morphing techniques were used to morph between their 2D representations. The 3D intermediate objects were thus reconstructed from the resulting 2D images. In 3D metamorphosis, Lazarus and Verroust [14] summarized and categorized all the algorithms in transformation between two shapes into two major approaches, volume based approaches and boundary based approaches.

The volume based approaches focus on interpolations between two shapes in voxel representation. Pasko and Savchenko [15] defined a metamorphosis between two general implicit surfaces by direct linear interpolation of the corresponding volumetric values. The method was entirely automatic but lacked the control over the transformation. Wyvill [16] presented a skeleton based approach to allow users to select pairs of corresponding skeletons. The transformation comprised several interpolations in associated potential fields or soft objects of paired skeletons. Kaul and Rossignac [17] developed an interpolation algorithm based on Minkowski sums of two sets of volumetric data. The method was further extended for transformation between a set of convex polyhedra using Bézier interpolation and Minkowski sums [18]. Galin and Akkouche [19] proposed an algorithm for soft objects built from skeletons of convex shapes, which was a mixed approach between skeleton and Minkowski sums. The paired skeletons were interpolated with Minkowski sums, and soft objects were blended by interpolations. Then the final interpolated shapes were the Minkowski sums between the interpolated soft objects and skeletons. Barbier et al. [20] extended Galin's work by removing the limitation to convex polygonal elements of arbitrary dimension. The new approach presented a vast variety of shapes including curves, surfaces, and volumes such as boxed or cone-spheres that may be used as skeletal elements.

Hughes [21] proposed an approach with interpolation of two shapes in the Fourier domain. The approach interpolates the low frequencies of the initial and end shapes while the high frequencies of the end shape are incrementally added in. The advantage of this approach is to avoid the shape distortion caused by direct interpolation of high frequency components. A similar approach was proposed by He et al. [22], but it was based on 3D wavelets. The initial volumetric data was decomposed with multiple levels of resolution, and the intermediate surfaces were reconstructed after interpolation of low frequencies. The spatial information within each frequency band of wavelets enabled a smooth transition.

To enable local controls, Lerios et al. [23] proposed a feature-based volume metamorphosis which allowed user to specify features in one shape corresponding to the other. These paired features can be transformed from one to the other during the morphing process. Cohen-Or and Levin [24] proposed a morphing algorithm based on three-dimensional distance field. The initial and end shapes were first deformed by some point-to-point warping functions which were designed to enforce topological correspondence and geometrical properties. The technique interpolates the distance values of each voxel and reconstructs the intermediate surfaces out of the intermediate distance field.

Turk and O'Brien [25] developed a metamorphosis scheme to transform between two shapes by creating a variational implicit function in a higher dimension after artificially introducing one extra dimension. Thus, the parallel slices based on the extra dimension represented the transformation sequence. Turk and O'Brien [26] further proposed another metamorphosis based on implicit surfaces creations. In this method, a set of constraints which were from scattered data of a surface created an implicit function. The transformation between two shapes was defined by the implicit surfaces built from the mixed constraints of the two shapes.

Various interpolation approaches have been developed. Fausett et al. [27] demonstrated a technique to transform between several 3D shapes of different topology by bi-linear interpolation in a higher dimensional space. Fang et al. [28] presented a continuous field based morphing algorithm. In this algorithm, a complex surface was construed by several polyhedral skeletons. Basic continuous field for each skeleton was created using variational interpolation. The intermediate surfaces between two shapes were approximated by the iso-

surface of the global field which is fused by the blended basic fields of the two shapes. Treece et al. [29] developed an algorithm to improve the transformation between two shapes by ensuring that no part of each surface remains disconnected during the morph. The morph was guided by correspondence of sphere representations of the two shapes, which was mapped from their distance field volume representations. Optimization-based approaches were also taken. Cong et al. [30] developed an approach for shape metamorphism under the constraints of initial and end surface functions. With the *p*-Laplacian equation, a series of regularized terms based on the gradient of the implicit function was generalized. The approach solves the time dependant implicit function which minimizes the supremum of the gradient during the morph. Bao et al. [31] presented a morphing process between two homeomorphic point-set surfaces by optimizing an energy function.

Among boundary based approaches, Sun et al. [32] proposed to interpolate polyhedral models using intrinsic shape parameters, such as dihedral angles and edge lengths. Lazarus and Verroust [33] developed a metamorphosis for cylinder-like objects by constructing polyhedral meshes using parameterization for two shapes. The parameters include 3D axes for discretization, vertices, edges and faces. The shape transformation was defined by the interpolation of the parameterization. Chen and Parent [34] introduced a user interactive algorithm to extract parameters form two 3D objects represented by planar contours. Weighted averaging of these parameters defined the shape transformation. Kanai et al. [35] presented an algorithm for 3D geometric metamorphosis between two objects based on harmonic map. 2D embeddings were created by harmonic map for the two 3D shapes with adjacent relations preserved. In-between shapes were created by merging of the two 2D embeddings.

Different from the above, the metamorphosis approach developed in this paper is based on the interpolation in the PS parameter space. This provides certain levels of control for our PS models. In addition, two smoothness criteria and one heuristic morphing method are proposed for pathway selection.

3. PERIODIC SURFACE

A periodic surface is generally defined as

$$\psi(\mathbf{r}) = \sum_{l=1}^{L}\sum_{m=1}^{M} \mu_{lm} \cos\left(2\pi\kappa_l(\mathbf{p}_m^T \cdot \mathbf{r})\right) = 0 \qquad (3.1)$$

where κ_l is the *scale parameter*, $\mathbf{p}_m = [a_m, b_m, c_m, \theta_m]^T$ is a *basis vector*, which represents a *basis plane* in the 3-space $\mathbb{E}^3$, $\mathbf{r} = [x, y, z, w]^T$ is the location vector with homogeneous coordinates, and μ_{lm} is the *periodic moment*. We usually assume $w = 1$ if not explicitly specified. It means the dimensions *x*, *y* and *z* are in the same scale. The *degree* of $\psi(\mathbf{r})$ in Eq.(3.1) is defined as the number of unique periodic basis vectors in set $\{\mathbf{p}_m\}$, $\deg(\psi(\mathbf{r})) := |\{\mathbf{p}_m\}|$. The *scale* of $\psi(\mathbf{r})$ is defined as the number of unique scale parameters in set $\{\kappa_l\}$, $\mathrm{sca}(\psi(\mathbf{r})) := |\{\kappa_l\}|$. We usually assume the scale parameters are natural numbers ($\kappa_l \in \mathbb{N}$). Each basis vector can be regarded as a set of parallel 2D subspaces in $\mathbb{E}^3$, which plays an important role in interactive manipulation of PS models.

The PS model described in Eq.(3.1) can also be represented by a PS parameter matrix as shown in Figure 3. The PS parameter matrix contains four sub-matrices ($\boldsymbol{\kappa}$, $\boldsymbol{\mu}$, $\mathbf{p}^T$ and $\mathbf{0}$). Each element μ_{lm} in $\boldsymbol{\mu}$ along with the *l*-th element κ_l in $\boldsymbol{\kappa}$ and the *m*-th row $\mathbf{p}_m^T$ in $\mathbf{p}^T$ defines a cosine function $\mu_{lm}\cos\left(2\pi\kappa_l(\mathbf{p}_m^T \cdot \mathbf{r})\right)$. Periodic surfaces are thus modeled by the sum of these *LM* cosine functions. Switching the first *L* columns or the last *M* rows of the PS parameter matrix does not change the periodic surface. There are totally $L!M!$ possible combinations of columns and rows in the sub-matrix $\boldsymbol{\mu}$, and $L!M!$ different PS parameter matrices represent the same periodic surface. This property is important when we apply interpolation in the PS parameter space, as discussed later in Section 4.2.

$$\left[\begin{array}{ccccc|c} \kappa_1 & \kappa_2 & \cdots & \cdots & \kappa_L & 0 \\ \hline \mu_{1M} & \mu_{2M} & \cdots & \cdots & \mu_{LM} & \mathbf{p}_M^T \\ \cdots & \cdots & \cdots & \cdots & \cdots & \cdots \\ \cdots & \cdots & \cdots & \cdots & \cdots & \cdots \\ \mu_{13} & \mu_{23} & \cdots & \cdots & \mu_{L3} & \mathbf{p}_3^T \\ \mu_{21} & \mu_{22} & \cdots & \cdots & \mu_{L2} & \mathbf{p}_2^T \\ \mu_{11} & \mu_{12} & \cdots & \cdots & \mu_{L1} & \mathbf{p}_1^T \end{array}\right] = \begin{bmatrix} \boldsymbol{\kappa} & \mathbf{0} \\ \boldsymbol{\mu} & \mathbf{p}^T \end{bmatrix}$$

M rows; *L* columns

Figure 3. PS parameter matrix

PS model is employed for surface creation because periodic structures are ubiquitous in natural materials. Crystal structures are one of the good examples that certain combinations of atoms are appeared periodically in the 3D space. Due to its periodic property, a closed-form equation is able to represent a periodic surface. Hence, it is an efficient tool for periodic structure modeling.

4. MORPHING SCHEMES

In this section, two morphing schemes are discussed. They are direct linear interpolation of volumetric data and interpolation in the PS parameter space. In the first method, volumetric data is generated by interpolating between those of the initial and the end surfaces. The intermediate surfaces are the isosurfaces based on the interpolated volumetric data. In the second method, linear interpolation is applied between the parameters of the initial and the end surfaces. Hence, the intermediate surfaces are created by closed-form PS models.

4.1 Volumetric Interpolation

Linear interpolation is widely used in geometric morphing process. It can be applied in the morphing of periodic surfaces. For the initial surface $\psi_1(\mathbf{r})=0$ and the end surface $\psi_2(\mathbf{r})=0$, volumetric interpolation between these two surfaces can be defined as $(1-\lambda)\psi_1(\mathbf{r})+\lambda\psi_2(\mathbf{r})=0$, where $\lambda\in[0,1]$. As an example, Figure 4 illustrates the effect of the interpolation between the P surface and I-WP surface. The PS parameter matrices for P surface and I-WP surfaces are shown as follows.

P surface parameter matrix:

$$\begin{bmatrix} 1 & 0 & 0 & 0 & 0 \\ 1 & 1 & 0 & 0 & 1 \\ 1 & 0 & 1 & 0 & 1 \\ 1 & 0 & 0 & 1 & 1 \end{bmatrix}$$

I-WP surface parameter matrix:

$$\begin{bmatrix} 1 & 0 & 0 & 0 & 0 \\ -1 & 2 & 0 & 0 & 1 \\ -1 & 0 & 2 & 0 & 1 \\ -1 & 0 & 0 & 2 & 1 \\ 1 & 1 & -1 & 0 & 1 \\ 1 & 1 & 1 & 0 & 1 \\ 1 & 0 & 1 & -1 & 1 \\ 1 & 0 & 1 & 1 & 1 \\ 1 & 1 & 0 & -1 & 1 \\ 1 & 1 & 0 & 1 & 1 \end{bmatrix}$$

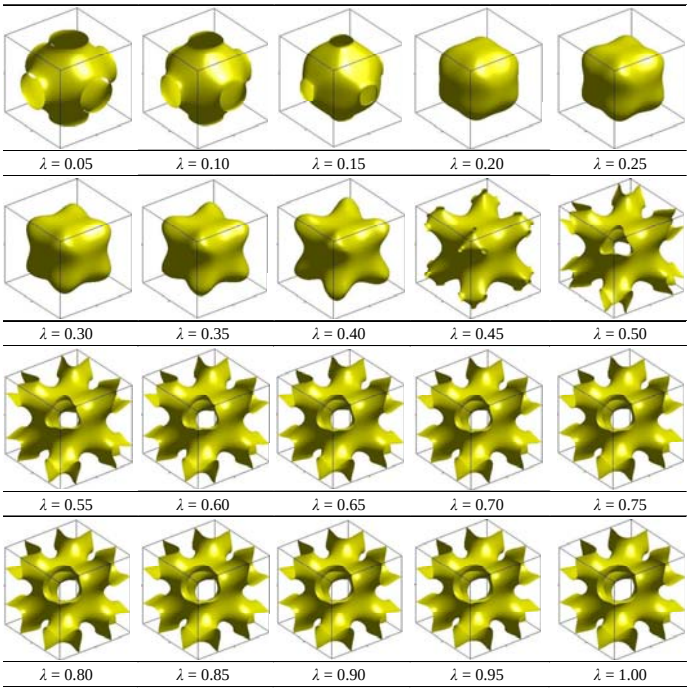

Figure 4. Linear interpolation between P surface and I-WP surface

The method of linear interpolation of volumetric data in the three dimensional space is straight forward. However, only one transition path is possible by applying this method if the initial and the end surfaces are known. There is no control over the transformation process because the transition path can not be locally modified. Creating correspondences between certain local regions is not possible. In addition, the surface transformation may not be continuous. For instance, in the example of Figure 4, the topology changes dramatically from $\lambda=0.15$ to $\lambda=0.20$. The six holes clearly as features vanish simultaneously in the intermediate surface. Similarly, the features of holes reappear in the intermediate surface when $\lambda=0.45$. The figure also shows that the transition path is hardly uniform because the topology changes more in the first half of the path than in the second half. To investigate more possible transition paths, the method of interpolation in the parameter space of PS modes is proposed in Section 4.2.

4.2 Interpolation in the parameter space of PS models

An alternative morphing scheme is to interpolate in the PS parameter space between the initial and the end surfaces. More specifically, for two surfaces

$$\psi_1(\mathbf{r})=\sum_{l=1}^{L_1}\sum_{m=1}^{M_1}\mu'_{lm}\cos\left(2\pi\kappa'_l(\mathbf{p}'^T_m\cdot\mathbf{r})\right)=0 \qquad (4.1)$$

$$\psi_2(\mathbf{r})=\sum_{l=1}^{L_2}\sum_{m=1}^{M_2}\mu''_{lm}\cos\left(2\pi\kappa''_l(\mathbf{p}''^T_m\cdot\mathbf{r})\right)=0 \qquad (4.2)$$

the interpolated surface is $\psi(\mathbf{r})=\sum_{l=1}^{L}\sum_{m=1}^{M}\mu_{lm}\cos\left(2\pi\kappa_l(\mathbf{p}_m^T\cdot\mathbf{r})\right)=0$, where

$$\begin{cases} \mu_{lm}=(1-\lambda)\mu'_{lm}+\lambda\mu''_{lm} \\ \kappa_l=(1-\lambda)\kappa'_l+\lambda\kappa''_l \\ \mathbf{p}_m=(1-\lambda)\mathbf{p}'_m+\lambda\mathbf{p}''_m \\ \lambda\in[0,1] \\ L=\max(L_1,L_2) \\ M=\max(M_1,M_2) \end{cases} \qquad (4.3)$$

In the PS parameter matrix form, let $\mathbf{A}=\begin{bmatrix}\boldsymbol{\kappa}' & \mathbf{0}\\ \boldsymbol{\mu}' & \mathbf{p}'\end{bmatrix}$ for $\psi_1(\mathbf{r})$ and $\mathbf{B}=\begin{bmatrix}\boldsymbol{\kappa}'' & \mathbf{0}\\ \boldsymbol{\mu}'' & \mathbf{p}''\end{bmatrix}$ for $\psi_2(\mathbf{r})$. The interpolation is also defined as $(1-\lambda)\mathbf{A}+\lambda\mathbf{B}$, where $\lambda\in[0,1]$. In other words, the interpolation is a process to linearly transform from one matrix to another, as illustrated in Figure 5.

Here, the PS parameter matrices of the initial and the end surfaces are to be extended to the same size before interpolation if they are in different sizes. Figure 6 illustrates the matrix extension. In Figure 6(a), if $L_1<L_2$ and $M_1<M_2$, the columns for the scale parameters κ's can be extended from L_1 to L_2, and the rows for the basis vectors can be

extended from M_1 to M_2 for surface $\psi_1(\mathbf{r})$ by setting $\mu'_{lm}=0$, $\kappa'_l=\kappa''_l$ and $\mathbf{p}'_m=\mathbf{p}''_m$ for $l\in[L_1+1,L_2]$ or $m\in[M_1+1,M_2]$. In Figure 6(b), if $L_1<L_2$ and $M_1>M_2$, the columns for scale parameters of surface $\psi_1(\mathbf{r})$ can be extended from L_1 to L_2 by setting $\mu'_{lm}=0$ and $\kappa'_l=\kappa''_l$ for $l\in[L_1+1,L_2]$. At the same time, the rows for basis vectors of surface $\psi_2(\mathbf{r})$ can be extended from M_2 to M_1 by setting $\mu''_{lm}=0$ and $\mathbf{p}''_m=\mathbf{p}'_m$ for $m\in[M_2+1,M_1]$.

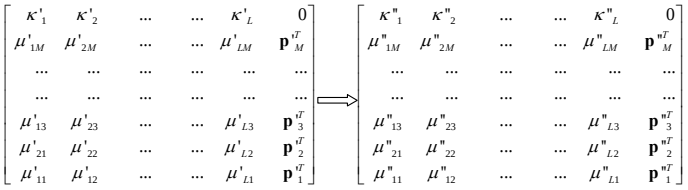

Figure 5. Matrix transformation

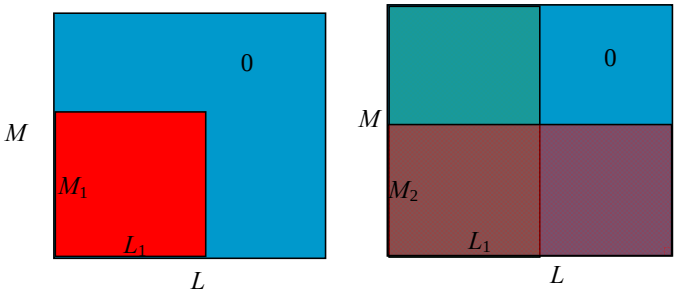

(a) (b)

Figure 6. Matrix extension

As mentioned in Section 3, switching rows or columns respectively within the last M rows or the first L columns of the PS parameter matrix does not change the periodic surface. However, it makes the interpolated periodic surfaces different when the method of interpolation in the PS parameter space is applied, as seen in Eq.(4.3). Thus, for two surfaces $\psi_1(\mathbf{r})$ in Eq.(4.1) and $\psi_2(\mathbf{r})$ in Eq.(4.2), there are possibly

$$\frac{\max(L_1,L_2)!\max(M_1,M_2)!}{|L_1-L_2|!|M_1-M_2|!}$$

different transition paths between the initial and end surfaces defined in Eq.(4.3). The objective is to select the "smoothest" transition path among all these potential candidates. Thus, quantitative criteria for smoothness are needed. In the next section, two smoothness criteria are proposed.

5. SMOOTHNESS CRITERIA

In this section, we propose two smoothness criteria, minimal space field change and minimal surface energy change, which will be described in Sec. 5.1 and Sec. 5.2, respectively. The first criterion is based on the potential energy point of view, which assumes the total change of space energy will be minimal during the morphing process. On the other hand, the second criterion is based on the surface energy point of view. It assumes the optimal transition paths will make the total change of surface energy minimal. In addition, a heuristic method of surface morphing is proposed in Sec. 5.3.

5.1 Minimal Space Field Change

In this criterion, it is assumed that the optimal transition path is the one with the minimal change of space field accumulatively during the morphing process. Since the volumetric values associated with PS models represent the potential energy in the three-dimensional space, the criterion of minimal space field change is to measure the total change of potential energy caused by the morphing process. Hence the transition path with the minimal total volumetric value change is considered to be the smoothest one. More accurately, in the domain $\mathbb{D}=[-0.5\le x\le 0.5,-0.5\le y\le 0.5,-0.5\le z\le 0.5,1]$, the *space field change* (SFC) between two periodic surfaces $\psi_a(\mathbf{r})$ and $\psi_b(\mathbf{r})$ is defined as $\mathrm{SFC}\triangleq\iiint_{\mathrm{D}}\left(\psi_b(\mathbf{r})-\psi_a(\mathbf{r})\right)^2 d\mathbf{r}$. Suppose $\psi_0(\mathbf{r})$ is the initial surface, $\psi_n(\mathbf{r})$ is the end surface and $\psi_k(\mathbf{r})$'s (k = 1, 2, …, n–1) are the n–1 intermediate surfaces, the total SFC (TSFC) is calculated by

$$\mathrm{TSFC}=\sum_{t=1}^{n}\iiint_{D}\left(\psi_t(\mathbf{r})-\psi_{t-1}(\mathbf{r})\right)^2 d\mathbf{r} \qquad (5.1)$$

Thus, the objective of this criterion is to minimize the TSFC.

In order to find the transition path with the minimal TSFC, we need to search and evaluate all possible candidates. The following example shows the morphing process from the P surface to I-WP surface using this criterion. Table 1 shows the corresponding PS parameter matrices of the P surface and I-WP surface after the matrix extension.

In this example, $L_1=L_2=1$, M_1 = 3 and M_2 = 9, as shown in Table 1. The degree of the P surface is extended to the same as that of the I-WP surface by setting $\mathbf{P}'_m=\mathbf{P}''_m$ and $\mu'_{1m}=0$, for $m=4,5,...,9$. The total number of the transition paths is $\frac{\max(1,1)!\max(3,9)!}{|1-1|!|3-9|!}=504$. For each of the n–1 intermediate frames (n=20) in the transition path, we calculate the sum square of volumetric value changes. A resolution of 100×100×100 in the discretized space is used. The TSFC is found according to Eq.(5.1) using step size 0.05. The optimal transition path is the one with the minimal TSFC. The best pair of PS parameter matrices based on this criterion is listed in Table 1. Figure 1 shows the optimal transformation sequence.

Table 1. The PS parameter matrices of P and I-WP surface for minimal space field change criterion

P surface	I-WP surface
$\begin{bmatrix} 1 & 0 & 0 & 0 & 0 \\ 1 & 1 & 0 & 0 & 1 \\ 1 & 0 & 1 & 0 & 1 \\ 1 & 0 & 0 & 1 & 1 \\ 0 & 1 & -1 & 0 & 1 \\ 0 & 0 & 2 & 0 & 1 \\ 0 & 0 & 1 & -1 & 1 \\ 0 & 0 & 1 & 1 & 1 \\ 0 & 2 & 0 & 0 & 1 \\ 0 & 0 & 0 & 2 & 1 \end{bmatrix}$	$\begin{bmatrix} 1 & 0 & 0 & 0 & 0 \\ 1 & 1 & 0 & -1 & 1 \\ 1 & 1 & 1 & 0 & 1 \\ 1 & 1 & 0 & 1 & 1 \\ 1 & 1 & -1 & 0 & 1 \\ -1 & 0 & 2 & 0 & 1 \\ 1 & 0 & 1 & -1 & 1 \\ 1 & 0 & 1 & 1 & 1 \\ -1 & 2 & 0 & 0 & 1 \\ -1 & 0 & 0 & 2 & 1 \end{bmatrix}$

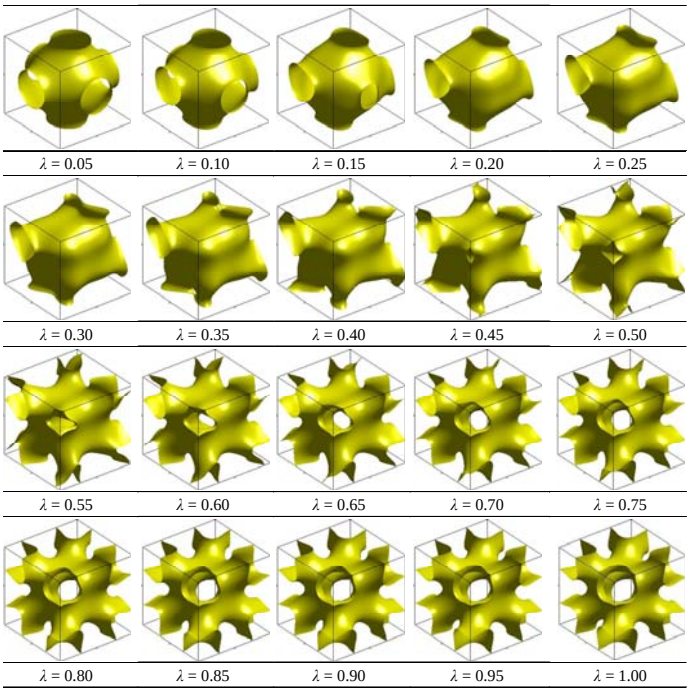

Figure 7. The optimal transition path based on minimal TSFC criterion

5.2 Minimal Surface Energy Change

Curvature in geometry is generally known as the amount by which a geometric object deviates from being flat. In differential geometry, surface energy can be defined as $E = \frac{1}{4}\int (k_1 + k_2)^2 dA$ where k_1 and k_2 are the two principle curvatures. In this criterion, we consider the Gaussian curvature of a periodic surface as an indicator of surface energy. Goldman [36] developed the curvature formulas for implicit surfaces. Therefore, for a periodic surface in Eq. (3.1), the Gaussian curvature can be calculated by

$$K = -\frac{\begin{vmatrix} H(\psi) & \nabla\psi^T \\ \nabla\psi & 0 \end{vmatrix}}{|\nabla\psi|^4} \qquad (5.2)$$

where $\nabla\psi$ is gradient and $H(\psi)$ is Hessian matrix.

It is assumed that the optimal transition path will make the accumulated change of surface energy minimal during the morphing. We map a periodic surface from its volumetric space into its surface energy space using Eq.(5.2) in the domain $\mathbb{D} = [-0.5 \le x \le 0.5, -0.5 \le y \le 0.5, -0.5 \le z \le 0.5, 1]$. The surface energy change (SEC) between two periodic surfaces $\psi_a(\mathbf{r})$ and $\psi_b(\mathbf{r})$ is defined as $\mathrm{SEC} \triangleq \iiint_{\mathrm{D}} \left(K_b(\mathbf{r}) - K_a(\mathbf{r})\right)^2 d\mathbf{r}$. Suppose that $\psi_0(\mathbf{r})$ is the initial periodic surface, $\psi_n(\mathbf{r})$ is the end periodic surface and $\psi_k(\mathbf{r})$'s (k = 1, 2, …, n–1) are the *n*–1 intermediate periodic surfaces. The total SEC (TSEC) is calculated by the Eq. (5.3). Thus, the objective of this criterion is to minimize the TSEC. In order to find the one with the minimal TSEC, we need to search and evaluate all the possible transition paths.

$$\mathrm{TSEC} = \sum_{t=1}^{n} \iiint_{D} \left(K_t(\mathbf{r}) - K_{t-1}(\mathbf{r})\right)^2 d\mathbf{r} \qquad (5.3)$$

Figure 8 shows the optimal morphing sequence from P surface to I-WP surface. In this example, a resolution of 50×50×50 in the discretized space is used. Step size is chosen as 0.20 so that the TSEC is based on the accumulated surface energy change of five surfaces or five steps. Table 2 lists the best pair of PS parameter matrices based on this criterion.

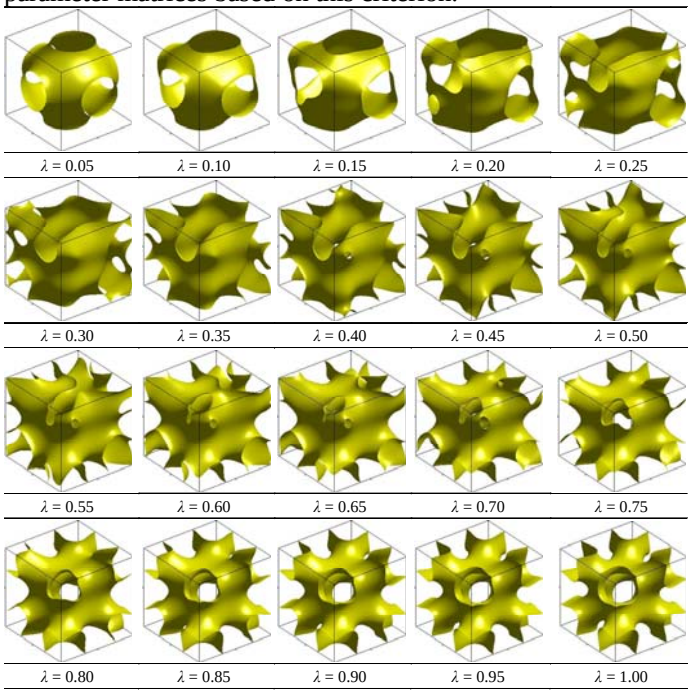

Figure 8. The optimal transition path based on minimal TSEC criterion

Table 2 The PS parameter matrices of P and I-WP surface for minimal surface energy change criterion

P surface	I-WP surface
$\begin{bmatrix} 1 & 0 & 0 & 0 & 0 \\ 1 & 1 & 0 & 0 & 1 \\ 1 & 0 & 1 & 0 & 1 \\ 1 & 0 & 0 & 1 & 1 \\ 0 & 1 & -1 & 0 & 1 \\ 0 & 1 & 1 & 0 & 1 \\ 0 & 2 & 0 & 0 & 1 \\ 0 & 0 & 2 & 0 & 1 \\ 0 & 0 & 0 & 2 & 1 \\ 0 & 1 & 0 & 1 & 1 \end{bmatrix}$	$\begin{bmatrix} 1 & 0 & 0 & 0 & 0 \\ 1 & 0 & 1 & -1 & 1 \\ 1 & 0 & 1 & 1 & 1 \\ 1 & 1 & 0 & -1 & 1 \\ 1 & 1 & -1 & 0 & 1 \\ 1 & 1 & 1 & 0 & 1 \\ -1 & 2 & 0 & 0 & 1 \\ -1 & 0 & 2 & 0 & 1 \\ -1 & 0 & 0 & 2 & 1 \\ 1 & 1 & 0 & 1 & 1 \end{bmatrix}$

5.3 Heuristic Morphing Criteria

The calculation of either minimal total change of space field or minimal total change of surface energy is a time consuming process, because the volumetric data or Gaussian curvature of all interpolated intermediate surfaces needs to be calculated in a volumetric domain for all possible transition paths. In this section, we propose a heuristic morphing criterion in the case of $L_1 = L_2 = 1$ and $\kappa'_1 = \kappa''_1 = 1$ in Eq. (4.1) and Eq. (4.2) for an easy-to-compute solution. In fact, the conditions of $L = 1$ and $\kappa = 1$ in Eq. (3.1) can always be met if we multiply all the scale parameters κ's with their corresponding $\mathbf{p}^T$'s to create new basis vectors. The purpose of this criterion is to reduce the time complexity to determine an acceptable smooth transition path by avoiding evaluations of all the intermediate surfaces. There are three assumptions behind the heuristic morphing criterion. First, since periodic moments $\mu's$ are the magnitude of cosine functions, they are considered to be scale related parameters. Second, since basis vectors $\mathbf{P}'s$ define the frequency and phase of cosine functions, they are considered to be shape related parameters. Finally, it is assumed that the morphing process is smooth if the changes of basis vectors are as little as possible. For two surfaces $\psi_1(\mathbf{r})$ and $\psi_2(\mathbf{r})$ in Eqs. (4.1) and (4.2) with $L_1 = L_2 = 1$ and $\kappa'_1 = \kappa''_1 = 1$, let $\mathbf{A} = \begin{bmatrix} \boldsymbol{\kappa}' & \mathbf{0} \\ \boldsymbol{\mu}' & \mathbf{p}' \end{bmatrix}$ for $\psi_1(\mathbf{r})$ and $\mathbf{B} = \begin{bmatrix} \boldsymbol{\kappa}'' & \mathbf{0} \\ \boldsymbol{\mu}'' & \mathbf{p}'' \end{bmatrix}$ for $\psi_2(\mathbf{r})$. Both $\mathbf{A}$ and $\mathbf{B}$ are $(M+1)\times 5$ matrices, where $M = \max(M_1, M_2)$. We generalize the heuristic morphing criterion as follows.

Step 1. For all the possible $\frac{M!}{|M_1 - M_2|!}$ transition paths, find the one with minimal $\sum_{m=1}^{M} |\mathbf{p}'_m - \mathbf{p}''_m|$.

Step 2. If more than one transition paths are found in step 1, further choose the one with minimal $\sum_{m=1}^{M_1} |\mathbf{p}''_m|$ if $M_1 < M_2$ or minimal $\sum_{m=1}^{M_2} |\mathbf{p}'_m|$ if $M_1 > M_2$.

Step 3. If more than one transition paths are found in step2, arbitrarily choose any one of them.

For the example to find a transition path from the P surface to I-WP surface, we apply this heuristic criterion. In step 1, 48 transition paths among the total of 504 possible transition paths are found. In step 2, 15 transition paths are further selected as candidates. Finally in step 3, we arbitrarily choose one transition path, as shown in Table 3. Figure 9 shows the heuristic transition path with the step size of 0.05.

Table 3 The PS parameter matrices of P and I-WP surface for heuristic morphing criterion

P surface	I-WP surface
$\begin{bmatrix} 1 & 0 & 0 & 0 & 0 \\ 1 & 1 & 0 & 0 & 1 \\ 1 & 0 & 1 & 0 & 1 \\ 1 & 0 & 0 & 1 & 1 \\ 0 & 0 & 0 & 2 & 1 \\ 0 & 0 & 2 & 0 & 1 \\ 0 & 0 & 1 & -1 & 1 \\ 0 & 1 & -1 & 0 & 1 \\ 0 & 1 & 0 & -1 & 1 \\ 0 & 2 & 0 & 0 & 1 \end{bmatrix}$	$\begin{bmatrix} 1 & 0 & 0 & 0 & 0 \\ 1 & 1 & 0 & 1 & 1 \\ 1 & 1 & 1 & 0 & 1 \\ 1 & 0 & 1 & 1 & 1 \\ -1 & 0 & 0 & 2 & 1 \\ -1 & 0 & 2 & 0 & 1 \\ 1 & 0 & 1 & -1 & 1 \\ 1 & 1 & -1 & 0 & 1 \\ 1 & 1 & 0 & -1 & 1 \\ -1 & 2 & 0 & 0 & 1 \end{bmatrix}$

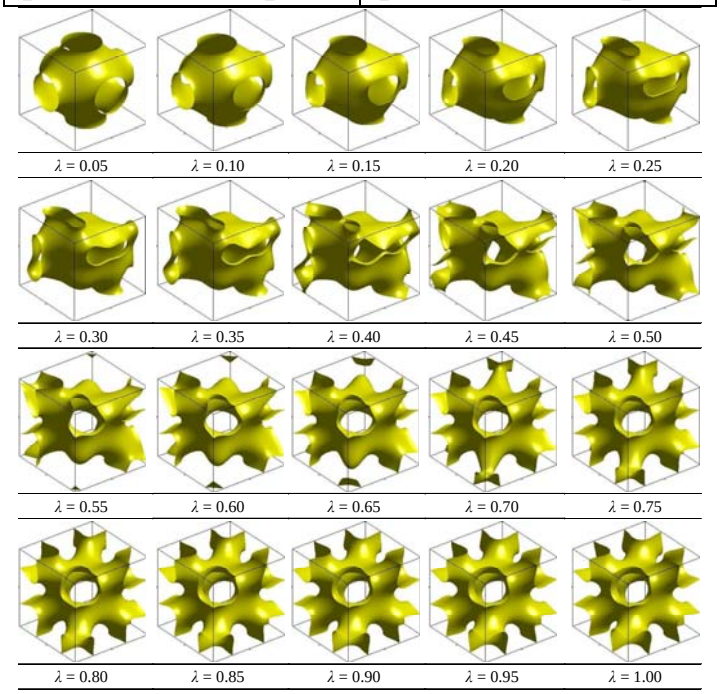

Figure 9. Heuristic morphing process from P surface to I-WP surface

5.4 Result discussions

We presented three quantitative smoothness criterions in this section and examples are given. Here, we only focus on metamorphosis of geometric aspect of a shape. Any physical conditions such as temperature which are possible to cause deviations between the actual transition path and the calculated optimal path are ignored in this stage. Since the type of phase transition that we are interested in is the movement of many atoms which results in changes between two crystal structures, it is reasonable to assume that all physical conditions like temperatures and pressures are uniform throughout the regions under consideration.

In the minimal space field change criteria, the best transition path is the one with the least change of field in the 3D space. Observing the shape transformation in Figure 7, we find the isosurfaces with isovalue zero in the transition path are reasonable to expect the minimal space field change subjectively. The minimal surface energy change criteria is to find the transition path which causes the least change of surface Gaussian curvature, an indicator of the degree of bend of a shape. According to the result shown in Figure 8, the shape transformation appears to be less change in surface bend than those in Figure 7 and Figure 9. The heuristic morphing criteria does not have physical interpretation, but it is faster in calculation than the other two because it is no need to calculate volumetric data for each possible transition path. The result shown in Figure 9 shows the shape transformation is reasonably smooth.

One of the advantages of these smoothness criteria is to provide a quantitative way so that the best transition path can be determined objectively. In addition, the method returns different outputs for different criteria. A proper selected criterion is needed only for selecting a transition path rather than another phase transition scheme. However, the major concern of the minimal space field change and surface energy change criteria is calculation efficiency because all possible alternative transitions must be evaluated before the optimal path can be concluded. A heuristic criterion is proposed for quick and acceptable solution, which may not be the optimum.

6. SUMMARY AND FUTURE WORK

The article presents a metamorphosis method between two PS models, using interpolation in the PS model parameters space. The parameter matrix representation of periodic surfaces is used so that the shape transformation is generated by matrix transformations. The metamorphosis of periodic surfaces creates multiple transition paths between two shapes. For further selections, different smoothness criteria are used to control the morphing process. Two smoothness criteria, the minimal space field change and the minimal space energy change, are proposed in this paper. To reduce calculation time, a heuristic criterion is also presented. The in-between shapes generated by the proposed method and smoothness criteria are natural and satisfactory.

One of the future extensions is to set up corresponding control points of the two periodic surfaces over the transformation. It may yield more smooth, hence more natural, transition path throughout the metamorphosis. Another potential extension is to add a fixed number of particles as a constraint during the morphing process. The consideration of the constraint will make it more realistic to material design.

ACKNOWLEDGEMENT

This work is supported in part by the NSF grant CMMI-0645070.

REFERENCES

[1] Wang, Y. (2006) Geometric modeling of nano structures with periodic surfaces. *Lecture Notes in Computer Science*, Vol.4077, pp.343-356

[2] Wang, Y. (2007) Periodic surface modeling for Computer Aided Nano Design. *Computer-Aided Design*, **39**(3): 179-189

[3] Wang, Y. (2007) Loci periodic surface reconstruction from crystals. *Computer-Aided Design & Applications*, **4**(1-4): 437-447

[4] Wang, Y. (2007) Degree operations on periodic surfaces. *Proc. 2007 IDETC/CIE Conference, Sept.4-7, 2007, Las Vegas, NV*, Paper No. DETC2007-35330

[5] Wang, Y. (2008) Degree elevation and reduction of periodic surfaces. *Computer-Aided Design & Applications*, in press

[6] Qi, C. and Wang, Y., (2008) Feature-Based Crystal Construction in Computer-Aided Nano-Design, *2008 ASME International Design Engineering Technical Conferences & The Computer and Information in Engineering Conference (IDETC/CIE2008), Aug.3-6, 2008, New York City, NY*, Paper No.DETC2008-49650

[7] Qi, C. and Wang, Y., (2008) Feature-Based Crystal Construction in Computer-Aided Nano-Design, *Computer-Aided Design*, in review

[8] Lasrado, V., Alhat, D., and Wang, Y., (2008) A Review of Recent Phase Transition Simulation Methods: Transition Path Search, *2008 ASME International Design Engineering Technical Conferences & The Computer and Information in Engineering Conference (IDETC/CIE2008), Aug.3-6, 2008, New York City, NY*, Paper No.DETC2008-49410

[9] Alhat, D., Lasrado, V., and Wang, Y., (2008) A Review of Recent Phase Transition Simulation Methods: Saddle Point Search, *2008 ASME International Design Engineering Technical Conferences & The Computer and Information in Engineering Conference (IDETC/CIE2008), Aug.3-6, 2008, New York City, NY*, Paper No.DETC2008-49411

[10] Wolberg, G. (1990) Digital Image Warping. *IEEE Computer Society P.*, Los Alamitos, CA

[11] Beier, T. and Neely, S. (1992) Feature-based image metamorphosis. *Computer Graphic*, vol 26(2), pp 35-43, New York, NY, July 1992

[12] Covell, M. and Withgott M. (1994) Spanning the gap between motion estimation and. *Proceedings of IEEE International Conference on Acoustics, Speech and Signal Processing*, vol 5, pp 213-216, New York, NY, 1994

[13] Mittal, A. (1999) Three-dimensional metamorphosis using multiplanar representation, *Multimedia Computing and Systems, IEEE International Conference*, Vol.1, pp:270-275

[14] Lazarus, F. and Verroust, A. (1998) Three-dimensional metamorphosis: a survey. *The Visual Computer*, 14:373-389

[15] Pasko, A. and Savchenko, V. (1995) Constructing functionally defined surfaces. *Implicit Surface*, Grenoble, France, Eurographics association, pp 97-106

[16] Wyvill, B. (1993) Modeling, visualizing and animating with implicit surfaces. *Metamorphosis of Implicit Surfaces (Siggraph'93 course notes Number 25)*, Anaheim, CA, USA, August 1993

[17] Kaul, A. and Rossignac, J. (1991) Establishing correspondences by topological merging: a new approach to 3-D shape transformation. *Graphics Interface'91*, Graphics Interface'91, Calgary, Canadian Information Processing Society, pp 271±278

[18] Rossignac, J. and Kaul, A. (1994) AGRELS and BIBs: metamorphosis as a Bezier curve in the space of polyhedra. *Eurographics'94*, Oslo, Blackwell, pp C179-184

[19] Galin, E. and Akkouche, S. (1996) Shape constrained blob metamorphosis. *Implicit Surface'96*, Poitiers, Blackwell, pp C143-C153

[20] Barbier, A., Galin, E. and Akkouche S. (2004) A framework of modeling, animating and morphing textured implicit models, *Graphical Models*, Volume 67, Issue 3, pp:166-188

[21] Hughes, J. (1992) Scheduled Fourier volume morphing. *Computer Graph (Siggraph'92)*, 26: 43-46

[22] He, T., Wang, S. and Kaufman, A. (1994) Wavelet-based volume morphing. *Proceedings of Visualization'94, IEEE Computer Society Press*, Washington, DC, pp 85-92

[23] Lerios, A., Garfinkle, C. and Levoy, M. (1995) Feature-based volume metamorphosis. *Computer Graph (SIGGRAPH' 95)* 29:449-464

[24] Cohen-Or, D., Levin, D. and Solomovoci, A. (1996) Contour blending using warp-guided distance field interpolation. *Proceedings of Visualization'96*, San Francisco, IEEE Computer Society Press, pp 165-172

[25] Turk, G., and O'Brien, J. (1999) Shape transformation using variational implicit functions, *Computer Graphics Proccedings, Annual Conference Serie' 99*, ACM SIGGRAPH'99, pp 335-342

[26] Turk, G., and O'Brien, J. (2002) Modelling with implicit surfaces that interpolate, *ACM Transactions on Graphics*, Vol.21, No.4, October 2002, pp 855-873

[27] Fausett E., Pasko A. and Adzhiev V., (2000) Space-time and higher dimensional modeling for animation, *Computer Animation 2000, IEEE Computer Society*, ISBN 0-7695-0683-6

[28] Fang, X., Bao, H., Heng, P., Wong, T. and Peng, Q., (2001) Continuous field based free-form surface modeling and morphing, *Computers & Graphics*, Vol. 25, Issue 2, April 2001, pp 235-243

[29] Treece, G., Prager, R. and Gee, A., (2001) Volume-based three-dimensional metamorphosis using sphere-guided region correspondence, *The Visual Computer*, 17: 397-414

[30] Cong, Ge., Esser, M., Parvin, B. and Bebis, G., (2004) Shape metamorphism using *p*-Laplacian equation, *Proceedings of the Pattern Recognition, 17th International Conference on (ICPR'04)*, Vol.04, pp 15-18

[31] Bao, Y., Guo, X. and Qin, H. (2005) Physically based morphing of point-sampled surfaces, *Computer Animation and Virtual Worlds*, 16: 509-418

[32] Sun, YM., Wang, W. and Chin, FY. (1997) Interpolating polyhedral models using intrinsic shape parameters. *Visualization Comput Anim*, 8:81-96

[33] Lazarus, F. and Verroust, A. (1997) Metamorphosis of cylinder-like objects. *Int J Visualization Comput Anim*, 8:131-146

[34] Chen, SE. and Parent, RE. (1989) Shape averaging and its applications to industrial design. *IEEE Comput Graph*, 9:47-54

[35] Kanai, T., Suzuki, H. and Kimura, F. (1998) 3D geometric metamorphosis based on harmonic map. An extended version of this paper appeared in the October issue of the Visual Computer. Visual Comput 14:166-176

[36] Goldman, R. (2005) Curvature formulas for implicit curves and surfaces, *Computer Aided Geometric Design*, 22:632–658